Geophysical Research Letters

RESEARCH LETTER
10.1029/2020GL089784

Key Points:
- Flux transfer event (FTE) showers (≥10 flux ropes in a magnetopause crossing) are prevalent when shear angle is large and plasma β is small
- FTE-type flux rope duration, spacing, core field, and flux content during shower events are shown to depend upon shear angle and plasma β
- FTE-type flux ropes in shower events carry between 60% and 85% of the magnetic flux required to supply Mercury's Dungey cycle

Supporting Information:
- Supporting Information S1
- Table S1

Correspondence to:
W. J. Sun,
wjsun@umich.edu

Citation:
Sun, W. J., Slavin, J. A., Smith, A. W., Dewey, R. M., Poh, G. K., Jia, X., et al. (2020). Flux transfer event showers at Mercury: Dependence on plasma β and magnetic shear and their contribution to the Dungey cycle. *Geophysical Research Letters*, *47*, e2020GL089784. https://doi.org/10.1029/2020GL089784

Received 8 JUL 2020
Accepted 6 OCT 2020
Accepted article online 17 OCT 2020

Flux Transfer Event Showers at Mercury: Dependence on Plasma β and Magnetic Shear and Their Contribution to the Dungey Cycle

W. J. Sun[1], J. A. Slavin[1], A. W. Smith[2], R. M. Dewey[1], G. K. Poh[3,4], X. Jia[1], J. M. Raines[1], S. Livi[1,5], Y. Saito[6], D. J. Gershman[4], G. A. DiBraccio[4], S. M. Imber[7], J. P. Guo[8], S. Y. Fu[9], Q. G. Zong[9], and J. T. Zhao[9]

[1]Department of Climate and Space Sciences and Engineering, University of Michigan, Ann Arbor, MI, USA, [2]Mullard Space Science Laboratory, University College London, Dorking, UK, [3]Center for Research and Exploration in Space Science and Technology II, Catholic University of America, Washington, D. C., USA, [4]Solar System Exploration Division, NASA Goddard Space Flight Center, Greenbelt, MD, USA, [5]South-West Research Institute, San Antonio, TX, USA, [6]Japan Aerospace Exploration Agency, Institute of Space and Astronautical Science, Kanagawa, Japan, [7]Department of Physics and Astronomy, University of Leicester, Leicester, UK, [8]School of Atmospheric Sciences, Sun Yat-sen University, Zhuhai, Guangdong, China, [9]School of Earth and Space Sciences, Peking University, Beijing, China

Abstract Mercury's flux transfer event (FTE) showers are dayside magnetopause crossings accompanied by large numbers (≥10) of magnetic flux ropes (FRs). These shower events are common, occurring during 52% (1,953/3,748) of the analyzed crossings. Shower events are observed with magnetic shear angles (θ) from 0° to 180° across the magnetopause and magnetosheath plasma β from 0.1 to 10 but are most prevalent for high θ and low plasma β. Individual FR duration correlates positively, while spacing correlates negatively, with θ and plasma β. FR flux content and core magnetic field intensity correlate negatively with plasma β, but they do not correlate with θ. During shower intervals, FRs carry 60% to 85% of the magnetic flux required to supply Mercury's Dungey cycle. The FTE showers and the large amount of magnetic flux carried by the FTE-type FRs appear quite different from observations at Earth and other planetary magnetospheres visited thus far.

Plain Language Summary Any planet with an interior dynamo will interact with the outward streaming stellar wind and likely form a magnetosphere. The magnetopause is a boundary between the shocked solar wind and planetary magnetic field, which can prevent most of the solar wind from directly entering into the magnetosphere. The multiple X-line reconnection that frequently occurs in the magnetopause creates helical magnetic fields that are termed magnetic flux ropes (FRs) about which open and interplanetary magnetic fields drape. FTE-type FRs generally have magnetic field lines with one end embedded in the solar wind and the other end connected to the planet through the magnetospheric cusp. The investigation of FTEs in Mercury's magnetosphere is of particular interest because they often occur in large numbers with extremely small temporal spacing, i.e., FTE showers, that are not seen elsewhere. We find that the properties of the FTE-type flux ropes in these showers depend upon plasma β in the magnetosheath and the magnetic shear angle across the magnetopause. The magnetic flux carried by these flux ropes dominates magnetic flux transfer between Mercury's dayside and nightside magnetosphere. These new results may contribute significantly to our understanding of solar wind-magnetosphere-exosphere coupling at Mercury.

1. Introduction

Mercury's global intrinsic magnetic field was discovered by Mariner 10 in the 1970s (Ness et al., 1974). Observations from MESSENGER confirm that Mercury's dipole moment is closely aligned with its rotation axis (<0.8°) with a magnitude of ~190 nT · R_M^3 (R_M is Mercury's radius, 2,440 km) and a northward offset of ~0.2 R_M (e.g., Alexeev et al., 2008; Anderson et al., 2008, 2012). The dipole magnetic field interacts with the solar wind to form a global magnetosphere that is a miniature in size compared with other planetary magnetospheres (e.g., Jackman et al., 2014; Slavin et al., 2007), with a subsolar magnetopause of only 1000 to 2000 kilometers above Mercury's surface (Siscoe et al., 1975; Slavin et al., 2008; Winslow et al., 2013).

FTEs are products of magnetic reconnection in the magnetopause current sheet between the interplanetary magnetic field (IMF) and the planetary magnetic field and are commonly observed at Earth (Haerendel et al., 1978; Russell & Elphic, 1978; Saunders et al., 1984), Mercury (Russell & Walker, 1985; Slavin et al., 2009), Jupiter (Walker & Russell, 1985), and Saturn (Jasinski et al., 2016). The magnetic field lines in FTEs have one end connected to the planet's cusp and the other to the solar wind, allowing magnetosheath and magnetosphere particles to mix in FTEs (e.g., Paschmann et al., 1982). In the core of FTEs, flux ropes (FRs) generated by multiple X-line reconnection are frequently observed (e.g., Lee & Fu, 1985). FTE-type FRs contain distinct bipolar variations in the magnetic field component normal to the magnetopause (B_N), which are coincident with enhancements in the magnetic field intensity (B_t). The magnetic flux concentrated in FTE-type FRs then convects tailward with the solar wind into the nightside magnetosphere and contributes to the magnetic flux circulation in the Dungey cycle (Dungey, 1961).

In the magnetospheres of Earth, Jupiter, and Saturn, FTE-type FRs have durations of around 1 min and spacings, i.e., repetition times, of 10 min (Jasinski et al., 2016; Lockwood et al., 1995; Walker & Russell, 1985). Their occurrence normally requires the magnetic shear angle (θ) between the magnetospheric magnetic field and IMF to be larger than 90° (e.g., Kuo et al., 1995), with large θ corresponding to shorter spacing (Wang et al., 2006). Furthermore, small magnetosheath plasma β (ratio of thermal pressure to magnetic pressure) is suggested to favor the occurrence of magnetopause magnetic reconnection (e.g., Ding et al., 1992; Scurry et al., 1994; Swisdak et al., 2010) and form FRs (e.g., Chen et al., 2019). FTE-type FRs at Earth contribute only a small fraction (<5%) of flux transported during the Dungey cycle's loading-unloading events (e.g., Rijnbeek et al., 1984).

At Mercury's dayside magnetopause, FTE-type FRs are more prevalent when θ is larger than 90° (Leyser et al., 2017). Sometimes, a large FTE-type FR (~0.06 MWb) could transport ~9% of the loaded flux in Mercury's loading-unloading events (Imber et al., 2014; Slavin, Lepping, et al., 2010). Furthermore, FTE-type FRs can appear extremely frequently with a spacing of ~10 s, which is known as an FTE shower (Slavin et al., 2012). Recently, several FTE showers were observed under the impact of coronal mass ejections, with one shower occurring under small θ (~60°) and low magnetosheath plasma β (~0.1) conditions (Slavin et al., 2014, 2019).

Due to its proximity to the Sun, Mercury experiences low solar wind Alfvénic Mach number (Slavin & Holzer, 1979). This condition often leads to a magnetosheath with low plasma β and a thick plasma depletion layer ahead of the dayside magnetopause (Gershman et al., 2013), which influences magnetopause reconnection (e.g., DiBraccio et al., 2013). Since FTE-type FRs are products of magnetopause reconnection, investigation into their dynamics could reveal features fundamental to magnetic reconnection. As FTE-type FRs repeat frequently at Mercury, the accumulated flux transport of these structures and their contribution to the overall flux circulation of the Dungey cycle is of great importance for our general understanding of Mercury's magnetosphere.

This study conducts a comprehensive investigation of FTE showers observed by MESSENGER at Mercury's dayside magnetopause. We present two FTE showers as examples, followed by a statistical investigation of 3,748 dayside magnetopause crossings. Our analysis shows that FTE showers are a common feature in Mercury's magnetosphere and that the occurrence and properties of FTE-type FRs depend on θ and magnetosheath plasma β. FTE-type FRs in the shower intervals can carry most of the flux that drives Mercury's Dungey cycle.

2. Flux Transfer Event Showers

2.1. Instrumentations and Data Sources

This study utilizes the magnetic field and proton measurements from MESSENGER (Solomon et al., 2007). The magnetic field data are from the magnetometer (Anderson et al., 2007), which have a time resolution of 50 ms and are displayed in Mercury solar magnetospheric coordinates (MSM). In MSM coordinates, $\hat{x}_{MSM}$ points from the center of Mercury's dipole to the Sun, $\hat{z}_{MSM}$ is anti-parallel to the dipole axis, and $\hat{y}_{MSM}$ completes the right-handed system, which is roughly against the orbital motion of Mercury. Spacecraft positions also have a time resolution of 50 ms, but the $\hat{x}_{MSM} - \hat{y}_{MSM}$ plane is rotated so that $\hat{x}_{MSM}$ is antiparallel to the average solar wind (400 km/s). The proton data are from the fast imaging plasma spectrometer (FIPS)

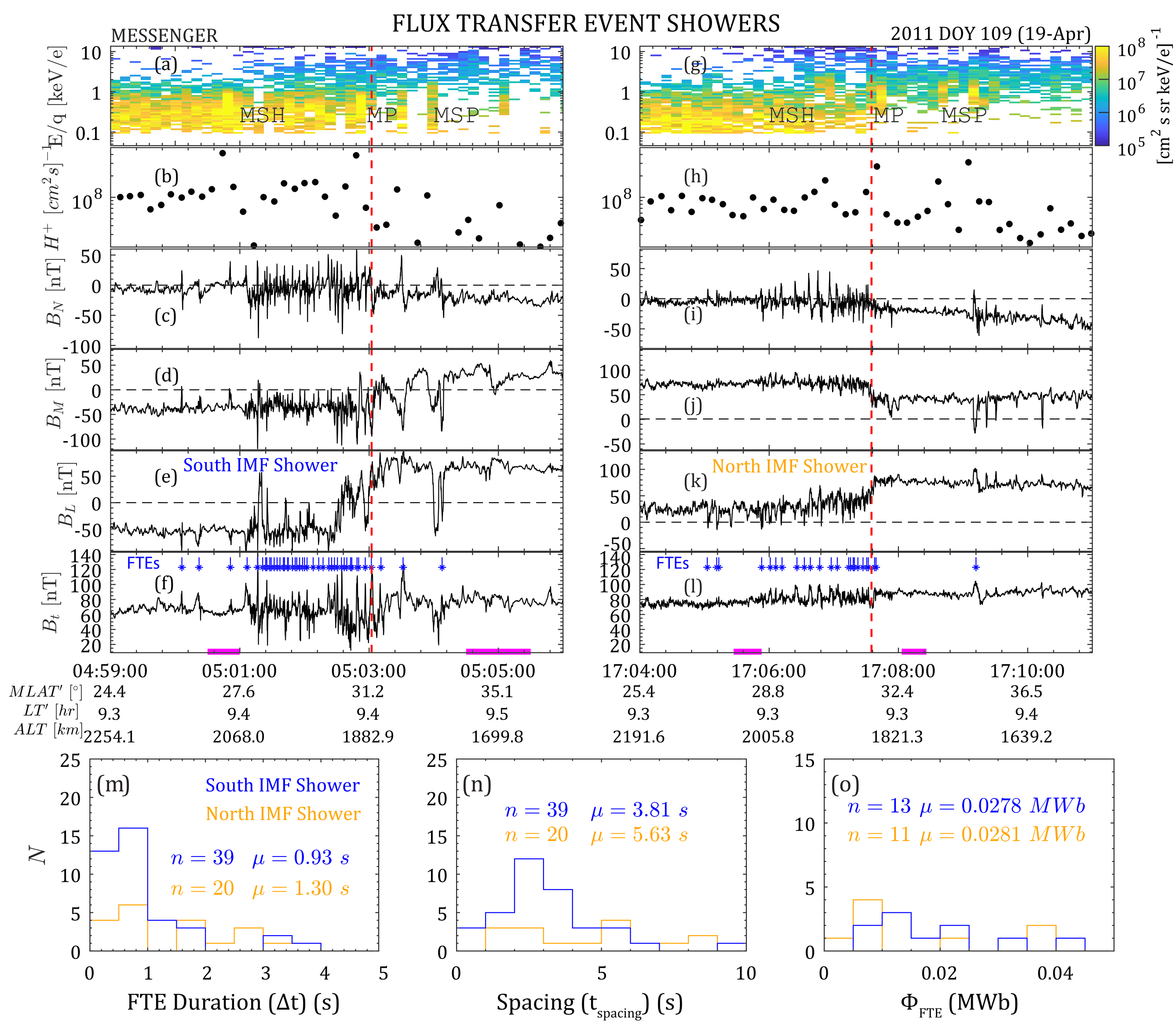

Figure 1. Overview of two flux transfer event (FTE) showers observed by MESSENGER on 19 April 2011. (a) to (f) is the South IMF Shower ($\widehat{N}$ = [0.84, −0.423, 0.41]), and (g) to (l) is the North IMF Shower ($\widehat{N}$ = [0.832, −0.435, 0.417]). (a) and (g) proton differential particle flux. (b) and (h) integrated proton particle flux. (c) and (i) B_N. (d) and (j) B_M. (e) and (k) B_L. (f) and (l) B_t, the blue lines ending with asterisks mark the FRs, the magenta bars mark the intervals used to obtain the average magnetic fields in the magnetosheath and the magnetosphere. The vertical dashed red lines indicate the average magnetopause locations. Magnetic field measurements in MSM coordinates are shown in the supplementary material. (m) FRs durations (Δt), (n) temporal spacing between neighboring FRs, and (o) axial magnetic flux content (Φ_{FTE}), n indicates the number of FRs, and μ indicates the mean values.

(Andrews et al., 2007), which measures proton fluxes in the energy range of ~50 eV/e to 13.3 keV/e at a scan time of ~10 s with an effective field of view of ~1.15π sr.

2.2. Two FTE Showers on 19 April 2011

On 19 April 2011, MESSENGER crossed the dayside magnetopause twice from the magnetosheath to the magnetosphere on the morning side (local time of ~09:20) at low magnetic latitude (~31.5°). The two magnetopause crossings were separated by ~12 h and, as shown in Figure 1, were accompanied by clear magnetic field rotations, decreases in low energy magnetosheath protons (<1 keV), and increases in high energy magnetospheric protons (>1 keV).

The first magnetopause crossing (Figures 1a–1f) occurred during southward IMF with θ ~177°. The magnetosheath plasma β was ~0.62, for which the magnetosheath thermal pressure is obtained by subtracting the magnetosheath magnetic pressure from the magnetospheric magnetic pressure adjacent to the magnetopause. This analysis assumes that the magnetospheric thermal pressure is much smaller than the magnetospheric magnetic pressure (see, DiBraccio et al., 2013) and quasi-pressure balance at the magnetopause. Even when magnetic reconnection occurs at the magnetopause, the magnetic pressure contributed from B_N is only 1% to 4% of the magnetospheric pressure since the reconnection rate is 0.1 to 0.2. Accordingly, this magnetic pressure due to B_N is small enough to be neglected. The second magnetopause crossing (Figures 1g–1l) corresponded to a northward IMF with θ ~28° and a magnetosheath plasma β of ~0.18. FTE-type FRs appeared in high frequencies during both magnetopause crossings, which we identify from their bipolar signatures in B_N coinciding with enhancements in B_t and containing clear magnetic field rotations (e.g., Slavin et al., 2009, 2012). The magnetopause normal ($\hat{N}$) is resolved from a magnetopause model (Shue et al., 1998; Winslow et al., 2013). $\hat{L}$ is perpendicular to $\hat{N}$ and in the plane determined by $\hat{N}$ and $\hat{z}_{MSM}$, and $\hat{M}$ completes the right-handed system.

2.3. FTE-Type FR Properties on 19 April 2011

Figures 1m–1o display FR properties of the two FTE showers. The FRs in the south and north IMF showers had mean durations (Δt) of 0.93 s and 1.3 s, respectively, for which Δt is determined from the B_N extrema. The average spacings ($t_{spacing}$), which are time separations between neighboring FR centers, are 3.8 s and 5.6 s, respectively.

Figure 1o displays a histogram of the axial magnetic flux contents of the FRs (Φ_{FTE}). The Φ_{FTE} is obtained through the Lundquist force-free FR model (Burlaga, 1988; Lepping et al., 1990; Lundquist, 1950), in which the plasma pressure across FR is assumed to be a constant, and the current density ($\vec{J}$) and magnetic field ($\vec{B}$) are parallel or antiparallel to each other ($\vec{J} \times \vec{B} = 0$). Lundquist (1950) introduced a solution of the magnetic field in cylindrical coordinates

$$\begin{cases} B_{axial} = B_{core} J_0(\alpha r/R_0) \\ \mathrm{B}_{azimuthal} = B_{core} H J_1(\alpha r/R_0), \\ B_{radial} = 0 \end{cases} \tag{1}$$

where B_{axial} is the axial magnetic field component, B_{core} is the core field, J_0 and J_1 are the zeroth and first-order Bessel functions, α equals 2.4048 (Burlaga, 1988), r is the distance to the flux rope center, R_0 is the flux rope radius, $B_{azimuthal}$ and B_{radial} are the azimuthal and radial magnetic field components, and H is the handedness (±1).

The FRs are modeled under their local coordinate system determined from minimum or maximum variance analysis (Sonnerup & Scheible, 1998), and their traveling speed is assumed to be 300 km/s. This assumption is made based on, first, the Alfvén speed in front of the magnetopause is typically between 300 and 400 km/s (Imber et al., 2014) and, second, the FTE traveling speed is between 100 and 500 km/s at Earth (Fear et al., 2017; Hasegawa et al., 2006). We further require a modified χ^2<0.05 for successful modeling (Smith, Slavin, Jackman, Poh, & Fear, 2017).

In the south and north IMF showers, 13 of 39 FTEs and 11 of 20 FTEs are successfully modeled. The mean Φ_{FTE} was ~0.028 MWb for both showers (Figure 1o), which is comparable to the values obtained in previous studies of Mercury's dayside FTEs (see, Slavin, Lepping, et al., 2010). We could satisfactorily model only a fraction of FTE-type FRs, which could imply that many of them were in their early stages and still contained enough plasma to affect their structure (see also Priest, 1990; Sun et al., 2019). The mean duration of magnetic flux loading-unloading event is determined to be 212 s with the loading duration of 115 s (T_{load}) (e.g., Imber & Slavin, 2017; Slavin, Anderson, et al., 2010; Sun et al., 2015). To estimate the flux transported by FRs within a loading event, we multiply the rate of FRs (i.e., T_{load} divided by the mean $t_{spacing}$) by the mean Φ_{FTE} to obtain the accumulated magnetic flux (Φ_{Flux}).

$$\Phi_{Flux} = T_{load} \Phi_{FTE} / t_{spacing}. \tag{2}$$

The Φ_{Flux} was around 0.84 MWb and 0.57 MWb for the two showers, which are both comparable to the loaded lobe open magnetic flux in a loading-unloading event (0.69 ± 0.38 MWb [Imber & Slavin, 2017]).

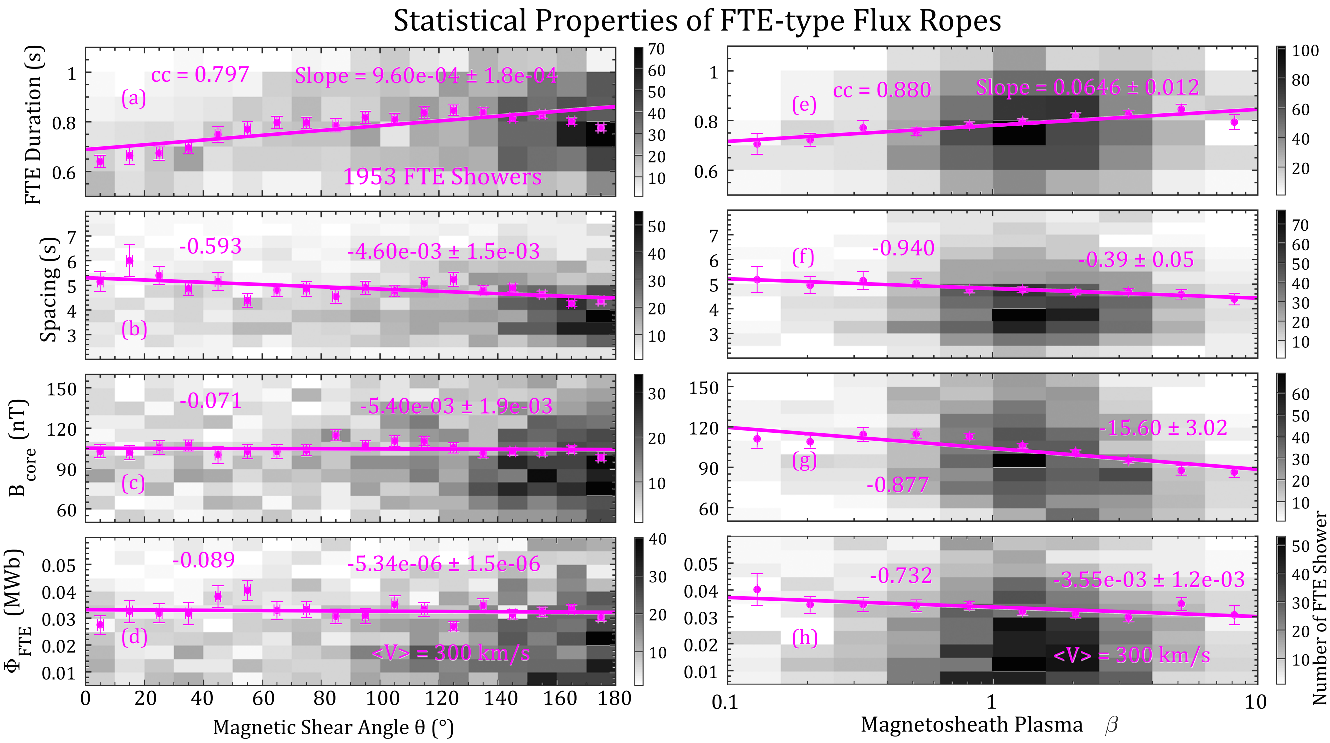

Figure 2. Statistical properties of FTE-type FRs (~73,000 FRs among 1953 FTE showers) as functions of the magnetic shear angle (θ) (a to d) and the magnetosheath plasma β (e to h). (a) and (e) duration Δt, (b) and (f) spacing, (c) and (g) maximum B_t (B_{max}) in FRs, (d) and (h) Φ_{FTE}. The colormap represents the number of shower events in each bin. The dots with error bars are the averages with standard errors in each interval. The standard errors include error propagation. The lines are the linear regression of the quantities with the slopes and correlation coefficients (cc) listed. Another version of scatter plots of this figure with event numbers in each bin is shown in the supporting information.

In this calculation, the mean Φ_{FTE} of all the FRs in the showers is assumed to be the mean Φ_{FTE} of those successfully modeled FRs.

3. Statistical Results on FTE Showers

3.1. FTE-Type FR Identification and Modeling

This section investigates Mercury's dayside magnetopause crossings made by MESSENGER from 11 March 2011 to 30 April 2015 (3,748 crossings). An established automatic FR detection technique (Smith, Slavin, Jackman, Fear, et al., 2017) applying the continuous wavelet transform (Daubechies, 1992) is employed to identify FTE-type FRs about those magnetopause crossings (2- to 4-min intervals). Details and applications on this automated FR technique can be found in Smith, Slavin, Jackman, Poh, and Fear (2017); Smith, Jackman, Frohmaier, Coxon, et al. (2018); Smith, Jackman, Frohmaier, Fear, et al. (2018). This study specifically requires FRs to contain bipolar B_N deflections coincident with both clear magnetic field rotations and enhancements in other components and B_t. A list of the dayside magnetopause crossings and more details on the selection of flux ropes can be found in the Supplementary Information.

Following FR selection, we apply the Lundquist force-free FR model to them to calculate their magnetic flux content. The speed of the FRs is assumed to be 300 km/s, and we require $\chi^2 < 0.05$ to be considered well-modeled.

3.2. Magnetosheath Plasma β and Magnetic Shear Dependency

Magnetopause crossings accompanied by 10 or more FTE-type FRs are identified as FTE showers. In the 3,748 magnetopauses included in the survey, 1,953 (~52%) were accompanied by FTE showers. The total number of FRs was ~73,000. Figure 2 shows the mean FR Δt, $t_{spacing}$, maximum B_t (B_{max}), and Φ_{FTE} dependencies on θ and magnetosheath plasma β for the 1953 showers. FTE showers occurred with θ from 0° to

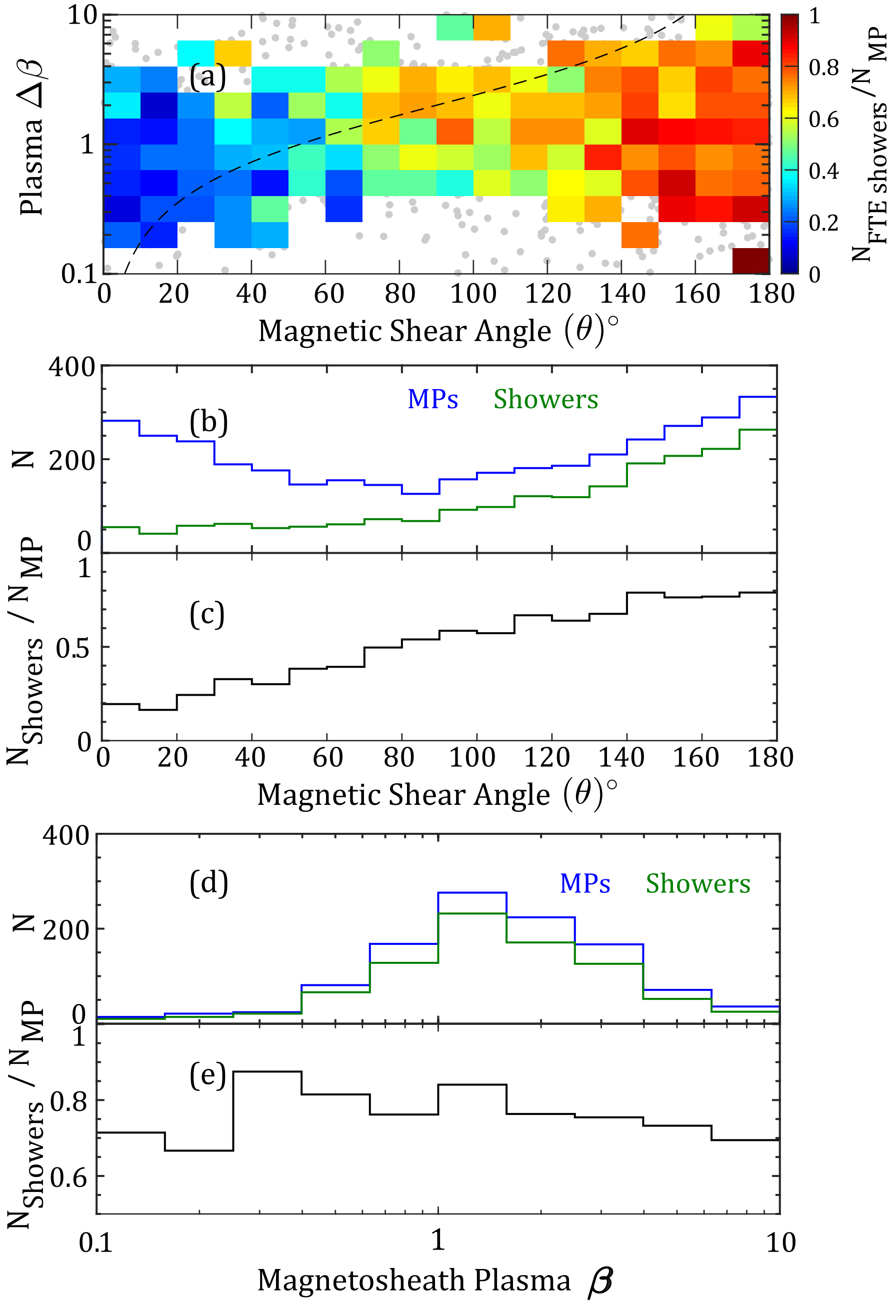

Figure 3. (a) Occurrence rates of FTE showers (1953) as functions of magnetic shear angle (θ) and plasma β difference ($\Delta\beta$) across the magnetopause, i.e., the number of FTE showers divided by the number of magnetopause crossings. Each bin requires at least five FTE showers or 10 magnetopause crossings. (b) numbers of magnetopause crossings (blue) and FTE showers (green). (c) occurrence rates of FTE showers along θ. (d) and (e) are along plasma β, which includes events in θ from 140° to 180°.

180° and plasma β from 0.1 to 10. FR Δt ranges from 0.5 to 1 s, $t_{spacing}$ from 3 to 7 s, B_{max} from 80 to 120 nT, and Φ_{FTE} from 0.02 to 0.05 MWb. We find Δt increases with increasing θ or plasma β. Spacing decreases with increasing θ and plasma β. In contrast, Φ_{FTE} and B_{max} do not clearly depend on θ, but they decrease with increasing plasma β.

Figure 3 shows the occurrence rates of FTE showers (i.e., percentage of magnetopause crossings with FTE showers) as functions of θ and plasma $\Delta\beta$. The plasma $\Delta\beta$ is the plasma β difference between magnetosheath and magnetosphere adjacent to the magnetopause, which is close to the magnetosheath plasma β.

10.1029/2020GL089784

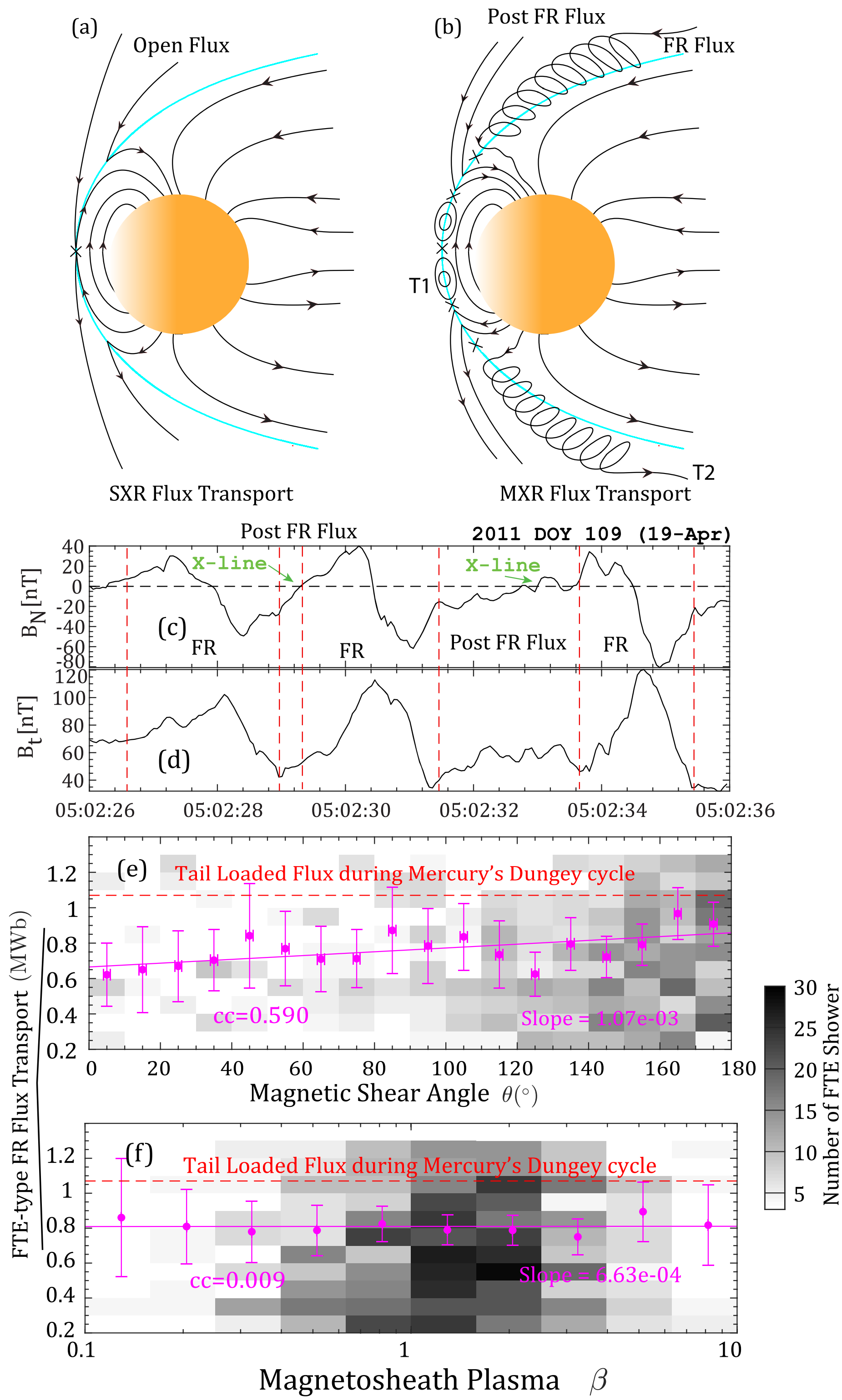

Figure 4. Schematic illustration of (a) Dungey's single X-line reconnection (SXR) flux transport and (b) multiple X-line reconnection (MXR) flux transport. (c) and (d) show examples of FTEs followed by post FTE flux from the shower event in Figure 1. (c) B_N, (d) B_t. (e) and (f) shows statistical features of 1953 FTE showers. The amount of flux carried by FTE-type FRs in the loading phase of Mercury's loading-unloading (115 s) as a function of magnetic shear angle (θ) (e) and magnetosheath plasma β (f). The dashed red lines indicate the loaded magnetic flux. The scatter plots of (e) and (f) are in the supporting information.

The percentages increase with increasing θ (Figures 3a and 3c), which are higher than 0.5 even for a small θ of ~70°. Furthermore, the percentages increase with decreasing plasma β in the large θ region from 140° to 180° (Figure 3e).

The curve in Figure 3a is a theoretical relation of plasma $\Delta\beta$ and θ (Swisdak et al., 2010),

$$\Delta\beta = 2\frac{L_{cs}}{\lambda_i}\tan\left(\frac{\theta}{2}\right), \tag{3}$$

where L_{cs} is thickness of current sheet and λ_i is the ion inertial length. Since magnetic reconnection normally requires L_{cs} to be comparable to λ_i to occur, L_{cs}/λ_i was set to unity. The theory predicts that the region below (above) the curve favors (suppresses) magnetic reconnection. The percentages are indeed high in large θ (> 120°) and small plasma $\Delta\beta$ region but are still low in small θ region (< 70°) even below the curve.

3.3. Contribution to Mercury's Dungey Cycle

FTE-type FRs are important elements for magnetic flux circulation in planetary magnetospheres. Dungey's initial model of reconnection was that single X-line reconnection (SXR) occurred on the dayside magnetopause and transported magnetic flux from the dayside to the nightside (Figure 4a, Dungey, 1961). Later, the multiple X-line reconnection (MXR) model was proposed to explain how magnetopause reconnection also concentrated reconnected flux into FRs (Figure 4b, Lee & Fu, 1985).

Outside of FTE-type FRs the open magnetic flux created by reconnection is expected to be found in the post-FR magnetopause current sheet (see Figure 4b), which is similar to the post-plasmoid plasma sheet observed in the tail. In the cross-tail current sheet, MXR creates a plasmoid-type flux rope while continued SXR reconnection creates a post-plasmoid plasma sheet composed of disconnected magnetic flux (Richardson et al., 1987; Slavin et al., 1993). Figures 4c and 4d display examples of post-FR reconnected flux between neighboring FRs in the MESSENGER observations during the 19 April 2011 shower. Here, B_N is directed normal to the magnetopause current sheet and is toward the planet (negative) in the northern hemisphere. It is difficult to accurately estimate the magnetic flux in the post-FR region since the spacecraft does not always remain in the magnetopause current sheet and the length of the reconnection X-lines are poorly constrained. Here, we make a rough estimation of the magnetic flux carried in the two post-FR regions. The averaged B_N values were −15.8 nT and −10.7 nT and were observed by MESSENGER for 0.4 s and 1.4 s, respectively. Assuming a flow speed of 300 km/s and an east–west X-line extent of 1 R_M, the magnetic fluxes were 0.005 MWb and 0.011 MWb in the two post-FR regions, which are each much smaller than the Φ_{FTE} in a single FTE-type FR (0.04 MWb).

Figures 4e and 4f show the magnetic flux carried by FTE-type FRs during the shower intervals on a timescale of a loading phase, which is calculated from Equation 2, as functions of θ and plasma β. The FTE-type FR transported magnetic flux are higher for large θ (~0.9 MWb) than small θ (~0.65 MWb) and had no clear dependency on plasma β (~0.8 MWb). The loaded magnetic flux is 1.07 MWb in Mercury's loading-unloading events (Imber & Slavin, 2017); therefore, FTE-type FRs in the shower intervals can transport between 60% and 85% of the magnetic flux needed for the Mercury's flux loading-unloading.

4. Discussion and Conclusions

This study utilized MESSENGER measurements to investigate FTE showers at Mercury's dayside magnetopause. FTE shower events (i.e., ≥10 FRs in a magnetopause crossing) are a common feature that accompanies around half (~52%) of all magnetopause crossings. FTE-type FR properties display clear dependencies on the magnetic shear angle and magnetosheath plasma β. FR durations are found to correlate positively with θ and plasma β; the larger the θ or β values, the longer the FR duration. However, FR spacing correlates negatively with θ and plasma β; the larger the θ or plasma β values, the more frequent the FRs. The maximum core magnetic field (B_{max}) and magnetic flux content (Φ_{FTE}) do not depend on θ but correlate negatively with plasma β. Furthermore, the percentage of magnetopause crossings with FTE showers correlates positively with θ but correlates negatively with plasma β. Overall, FTE-type FRs in shower intervals could carry between 60% and 85% of the magnetic flux for the flux circulation in Mercury's loading-unloading events. These results indicate that both θ and plasma β influence the occurrence of

FTEs and therefore the frequency of magnetopause reconnection, which is consistent with reconnection modeling by Swisdak et al. (2010). However, the effect of plasma β is prominent in the high θ region but not in the low θ region.

Many studies at Earth have shown that FTE-type FRs are responsible for <5% of the flux transported during the Dungey cycle (Fear et al., 2017; Rijnbeek et al., 1984). Rather, it is magnetic flux opened by single X-line reconnection and not associated with any FRs that dominates Earth's flux transport. Jupiter's and Saturn's magnetospheres have far fewer FTEs and they appear to carry a negligible amount of magnetic flux during the Dungey cycle (e.g., Jasinski et al., 2016; Walker & Russell, 1985). In contrast, Slavin, Lepping, et al. (2010) and Imber et al. (2014) show that a single large-scale FTE-type FR can sometimes carry a large portion (~9%) of the total magnetic flux transferred during Mercury's loading-unloading cycle. We utilize a much larger database of FTE-type FRs during shower events when the flux ropes are smaller in diameter and carry less magnetic flux individually. However, due to their abundance, these small FRs supply 60–85% of the magnetic flux circulation.

This result also implies that the less well studied, post-FR open flux, shown in Figure 4, contributes only a minor part of the total flux circulation, i.e., less than 15–40%. However, Fear et al. (2019) recently argued that magnetic flux outside of the FR core of the FTE could transfer several times the flux content of FRs, though they did conclude that the total flux carried by the FTE, i.e., the FR core and the post-FR magnetic flux, is the dominant supply for Mercury's Dungey cycle. Further, it should be noted that we have assumed the amplitude of the flux loading-unloading cycle at Mercury to be 1.07 MWb, which is the upper limit of 0.69 ± 0.38 MWb obtained by Imber and Slavin (2017). The reasons for taking the upper limit for the amplitude are that (1) the magnetic field might be amplified when magnetic flux tube is transported from the dayside into the nightside magnetosphere (Heyner et al., 2016) and (2) the flaring of Mercury's tail magnetopause and the magnetic flux transport in the quiet plasma sheet (Dewey et al., 2018) were not taken into account by Imber and Slavin (2017).

This study offers many clues to understanding magnetic reconnection at other magnetospheres under intense external driving, including moons of the giant planets such as Ganymede (Kivelson et al., 1996) and exoplanets that orbit close to their stars (Barclay et al., 2013). Ganymede is embedded within the sub-Alfvénic corotation flow in Jupiter's magnetosphere (e.g., Jia et al., 2008). FRs have been found to occur with similarly short spacings (tens of seconds) in global simulations of Ganymede's magnetosphere, including resistive MHD simulations (Jia et al., 2010) and hall MHD with embedded particle-in-cell simulations (Zhou et al., 2019).

The BepiColombo mission (Benkhoff et al., 2010) consists of two spacecraft, the Mercury Planetary Orbiter and Mercury Magnetospheric Orbiter, and is scheduled to arrive at Mercury in late 2025. BepiColombo will provide high-resolution magnetic field (Baumjohann et al., 2010; Glassmeier et al., 2010) and plasma measurements (Saito et al., 2010). At times, one spacecraft will serve as a solar wind monitor while the other is inside the magnetosphere. We can capitalize on using these dual-spacecraft observations to definitively determine the role of FTEs in forcing Mercury's dynamic magnetosphere and the solar wind drivers of FTE showers.

Acknowledgments

MESSENGER data used in this study were available from the Planetary Data System (PDS; http://pds.jpl.nasa.gov). The MESSENGER project was supported by the NASA Discovery Program under contracts NASW-00002 to the Carnegie Institution of Washington and NAS5-97271 to The Johns Hopkins University Applied Physics Laboratory. W. J. S. and J. A. S. were supported by NASA grants NNX16AJ67G and 80NSSC18K1137. A. W. S. was supported by STFC consolidated grant ST/S000240/1 and NERC grant NE/P017150/1. R. M. D. was supported by NASA's Earth and Space Science Fellowship Program (80NSSC17K0493). The magnetopause crossings along with local coordinates are available in the table named “DaysideMagnetopause_List.txt” in the supporting information.

References

Alexeev, I. I., Belenkaya, E. S., Bobrovnikov, S. Y., Slavin, J. A., & Sarantos, M. (2008). Paraboloid model of Mercury's magnetosphere. *Journal of Geophysical Research*, *113*, A12210. https://doi.org/10.1029/2008JA013368

Anderson, B. J., Acuña, M. H., Korth, H., Purucker, M. E., Johnson, C. L., Slavin, J. A., et al. (2008). The structure of Mercury's magnetic field from MESSENGER's first flyby. *Science*, *321*(5885), 82–85. https://doi.org/10.1126/science.1159081

Anderson, B. J., Acuña, M. H., Lohr, D. A., Scheifele, J., Raval, A., Korth, H., & Slavin, J. A. (2007). The magnetometer instrument on MESSENGER. *Space Science Reviews*, *131*(1–4), 417–450. https://doi.org/10.1007/s11214-007-9246-7

Anderson, B. J., Johnson, C. L., Korth, H., Winslow, R. M., Borovsky, J. E., Purucker, M. E., et al. (2012). Low-degree structure in Mercury's planetary magnetic field. *Journal of Geophysical Research*, *117*, E00L12. https://doi.org/10.1029/2012JE004159

Andrews, G. B., Zurbuchen, T. H., Mauk, B. H., Malcom, H., Fisk, L. A., Gloeckler, G., et al. (2007). The energetic particle and plasma spectrometer instrument on the MESSENGER spacecraft. *Space Science Reviews*, *131*(1–4), 523–556. https://doi.org/10.1007/s11214-007-9272-5

Barclay, T., Rowe, J. F., Lissauer, J. J., Huber, D., Fressin, F., Howell, S. B., et al. (2013). A sub-Mercury-sized exoplanet. *Nature*, *494*, 452–454. https://doi.org/10.1038/nature11914

Baumjohann, W., Matsuoka, A., Magnes, W., Glassmeier, K. H., Nakamura, R., Biernat, H., et al. (2010). Magnetic field investigation of Mercury's magnetosphere and the inner heliosphere by MMO/MGF. *Planetary and Space Science*, *58*(1–2), 279–286. https://doi.org/10.1016/j.pss.2008.05.019

Benkhoff, J., van Casteren, J., Hayakawa, H., Fujimoto, M., Laakso, H., Novara, M., et al. (2010). BepiColombo—Comprehensive exploration of Mercury: Mission overview and science goals. *Planetary and Space Science*, *58*(1–2), 2–20. https://doi.org/10.1016/j.pss.2009.09.020

Burlaga, L. F. (1988). Magnetic clouds and force-free fields with constant alpha. *Journal of Geophysical Research*, *93*(A7), 7217–7224. https://doi.org/10.1029/JA093iA07p07217

Chen, C., Sun, T. R., Wang, C., Huang, Z. H., Tang, B. B., & Guo, X. C. (2019). The effect of solar wind Mach numbers on the occurrence rate of flux transfer events at the dayside magnetopause. *Geophysical Research Letters*, *46*, 4106–4113. https://doi.org/10.1029/2018GL081676

Daubechies, I. (1992). *Ten Lectures on Wavelets* (Vol. 61). Philadelphia, Pa: SIAM.

Dewey, R. M., Raines, J. M., Sun, W., Slavin, J. A., & Poh, G. (2018). MESSENGER observations of fast plasma flows in Mercury's magnetotail. *Geophysical Research Letters*, *45*, 10,110–10,118. https://doi.org/10.1029/2018GL079056

DiBraccio, G. A., Slavin, J. A., Boardsen, S. A., Anderson, B. J., Korth, H., Zurbuchen, T. H., et al. (2013). MESSENGER observations of magnetopause structure and dynamics at Mercury. *Journal of Geophysical Research: Space Physics*, *118*, 997–1008. https://doi.org/10.1002/jgra.50123

Ding, D. Q., Lee, L. C., & Kennel, C. F. (1992). The beta dependence of the collisionless tearing instability at the dayside magnetopause. *Journal of Geophysical Research*, *97*(A6), 8257–8267. https://doi.org/10.1029/92JA00431

Dungey, J. W. (1961). Interplanetary magnetic field and the Auroral zones. *Physical Review Letters*, *6*(2), 47–48. https://doi.org/10.1103/PhysRevLett.6.47

Fear, R. C., Coxon, J. C., & Jackman, C. M. (2019). The contribution of flux transfer events to Mercury's Dungey cycle. *Geophysical Research Letters*, *46*, 14,239–14,246. https://doi.org/10.1029/2019GL085399

Fear, R. C., Trenchi, L., Coxon, J. C., & Milan, S. E. (2017). How much flux does a flux transfer event transfer? *Journal of Geophysical Research: Space Physics*, *122*, 12,310–12,327. https://doi.org/10.1002/2017JA024730

Gershman, D. J., Slavin, J. A., Raines, J. M., Zurbuchen, T. H., Anderson, B. J., Korth, H., et al. (2013). Magnetic flux pileup and plasma depletion in Mercury's subsolar magnetosheath. *Journal of Geophysical Research: Space Physics*, *118*, 7181–7199. https://doi.org/10.1002/2013JA019244

Glassmeier, K. H., Auster, H. U., Heyner, D., Okrafka, K., Carr, C., Berghofer, G., et al. (2010). The fluxgate magnetometer of the BepiColombo Mercury planetary orbiter. *Planetary and Space Science*, *58*(1–2), 287–299. https://doi.org/10.1016/j.pss.2008.06.018

Haerendel, G., Paschmann, G., Sckopke, N., Rosenbauer, H., & Hedgecock, P. C. (1978). The frontside boundary layer of the magnetosphere and the problem of reconnection. *Journal of Geophysical Research*, *83*(A7), 3195–3216. https://doi.org/10.1029/JA083iA07p03195

Hasegawa, H., Sonnerup, B. U. Ö., Owen, C. J., Klecker, B., Paschmann, G., Balogh, A., & Rème, H. (2006). The structure of flux transfer events recovered from cluster data. *Annales de Geophysique*, *24*(2), 603–618. https://doi.org/10.5194/angeo-24-603-2006

Heyner, D., Nabert, C., Liebert, E., & Glassmeier, K.-H. (2016). Concerning reconnection-induction balance at the magnetopause of Mercury. *Journal of Geophysical Research: Space Physics*, *121*, 2935–2961. https://doi.org/10.1002/2015JA021484

Imber, S. M., & Slavin, J. A. (2017). MESSENGER observations of magnetotail loading and unloading: Implications for substorms at Mercury. *Journal of Geophysical Research: Space Physics*, *122*, 11,402–11,412. https://doi.org/10.1002/2017JA024332

Imber, S. M., Slavin, J. A., Boardsen, S. A., Anderson, B. J., Korth, H., McNutt, R. L. Jr., & Solomon, S. C. (2014). MESSENGER observations of large dayside flux transfer events: Do they drive Mercury's substorm cycle? *Journal of Geophysical Research: Space Physics*, *119*, 5613–5623. https://doi.org/10.1002/2014JA019884

Jackman, C. M., Arridge, C. S., André, N., Bagenal, F., Birn, J., Freeman, M. P., et al. (2014). Large-scale structure and dynamics of the magnetotails of Mercury, Earth, Jupiter and Saturn. *Space Science Reviews*, *182*(1–4), 85–154. https://doi.org/10.1007/s11214-014-0060-8

Jasinski, J. M., Slavin, J. A., Arridge, C. S., Poh, G., Jia, X., Sergis, N., et al. (2016). Flux transfer event observation at Saturn's dayside magnetopause by the Cassini spacecraft. *Geophysical Research Letters*, *43*, 6713–6723. https://doi.org/10.1002/2016GL069260

Jia, X., Walker, R. J., Kivelson, M. G., Khurana, K. K., & Linker, J. A. (2008). Three-dimensional MHD simulations of Ganymede's magnetosphere. *Journal of Geophysical Research*, *113*, A06212. https://doi.org/10.1029/2007JA012748

Jia, X., Walker, R. J., Kivelson, M. G., Khurana, K. K., & Linker, J. A. (2010). Dynamics of Ganymede's magnetopause: Intermittent reconnection under steady external conditions. *Journal of Geophysical Research*, *115*, A12202. https://doi.org/10.1029/2010JA015771

Kivelson, M. G., Khurana, K. K., Russell, C. T., Walker, R. J., Warnecke, J., Coroniti, F. V., et al. (1996). Discovery of Ganymede's magnetic field by the Galileo spacecraft. *Nature*, *384*(6609), 537–541. https://doi.org/10.1038/384537a0

Kuo, H., Russell, C. T., & Le, G. (1995). Statistical studies of flux transfer events. *Journal of Geophysical Research*, *100*(A3), 3513–3519. https://doi.org/10.1029/94JA02498

Lee, L. C., & Fu, Z. F. (1985). A theory of magnetic flux transfer at the Earth's magnetopause. *Geophysical Research Letters*, *12*(2), 105–108. https://doi.org/10.1029/GL012i002p00105

Lepping, R. P., Jones, J. A., & Burlaga, L. F. (1990). Magnetic field structure of interplanetary magnetic clouds at 1 AU. *Journal of Geophysical Research*, *95*(A8), 11,957–11,965. https://doi.org/10.1029/JA095iA08p11957

Leyser, R. P., Imber, S. M., Milan, S. E., & Slavin, J. A. (2017). The influence of IMF clock angle on dayside flux transfer events at Mercury. *Geophysical Research Letters*, *44*, 10,829–10,837. https://doi.org/10.1002/2017GL074858

Lockwood, M., Cowley, S. W. H., Smith, M. F., Rijnbeek, R. P., & Elphic, R. C. (1995). The contribution of flux transfer events to convection. *Geophysical Research Letters*, *22*(10), 1185–1188. https://doi.org/10.1029/95GL01008

Lundquist, S. (1950). Magnetohydrostatic fields. *Arkiv foer Physik*, *2*, 361–365.

Ness, N. F., Behannon, K. W., Lepping, R. P., Whang, Y. C., & Schatten, K. H. (1974). Magnetic field observations near Mercury: Preliminary results from Mariner 10. *Science*, *185*(4146), 151–160. https://doi.org/10.1126/science.185.4146.151

Paschmann, G., Haerendel, G., Papamastorakis, I., Sckopke, N., Bame, S. J., Gosling, J. T., & Russell, C. T. (1982). Plasma and magnetic field characteristics of magnetic flux transfer events. *Journal of Geophysical Research*, *87*(A4), 2159–2168. https://doi.org/10.1029/JA087iA04p02159

Priest, E. R. (1990). The equilibrium of magnetic flux ropes. In C. T. Russell, E. R. Priest, L. C. Lee (Eds.), *Physics of magnetic flux ropes*, *Geophysical Monograph Series* (Vol. 58, pp. 1–22). Washington, DC: AGU.

Richardson, I. G., Cowley, S. W. H., Hones, E. W., & Bame, S. J. (1987). Plasmoid-associated energetic ion bursts in the deep geomagnetic tail: Properties of plasmoids and the postplasmoid plasma sheet. *Journal of Geophysical Research*, *92*(A9), 9997–10,013. https://doi.org/10.1029/JA092iA09p09997

Rijnbeek, R. P., Cowley, S. W. H., Southwood, D. J., & Russell, C. T. (1984). A survey of dayside flux transfer events observed by ISEE 1 and 2 magnetometers. *Journal of Geophysical Research*, *89*(A2), 786–800. https://doi.org/10.1029/JA089iA02p00786

Russell, C. T., & Elphic, R. C. (1978). Initial ISEE magnetometer results: Magnetopause observations. *Space Science Reviews*, *22*(6), 681–715. https://doi.org/10.1007/BF00212619

Russell, C. T., & Walker, R. J. (1985). Flux transfer events at Mercury. *Journal of Geophysical Research*, *90*(A11), 11,067–11,074. https://doi.org/10.1029/JA090iA11p11067

Saito, Y., Sauvaud, J., Hirahara, M., Barabash, S., Delcourt, D., Takashima, T., & Asamura, K. (2010). Scientific objectives and instrumentation of Mercury plasma particle experiment (MPPE) onboard MMO. *Planetary and Space Science*, *58*(1–2), 182–200. https://doi.org/10.1016/j.pss.2008.06.003

Saunders, M. A., Russell, C. T., & Sckopke, N. (1984). Flux transfer events: Scale size and interior structure. *Geophysical Research Letters*, *11*(2), 131–134. https://doi.org/10.1029/GL011i002p00131

Scurry, L., Russell, C. T., & Gosling, J. T. (1994). Geomagnetic activity and the beta dependence of the dayside reconnection rate. *Journal of Geophysical Research*, *99*(A8), 14,811–14,814. https://doi.org/10.1029/94JA00794

Shue, J.-H., Song, P., Russell, C. T., Steinberg, J. T., Chao, J. K., Zastenker, G., et al. (1998). Magnetopause location under extreme solar wind conditions. *Journal of Geophysical Research*, *103*(A8), 17,691–17,700. https://doi.org/10.1029/98JA01103

Siscoe, G. L., Ness, N. F., & Yeates, C. M. (1975). Substorms on Mercury? *Journal of Geophysical Research (1896–1977)*, *80*(31), 4359–4363. https://doi.org/10.1029/JA080i031p04359

Slavin, J. A., Acuña, M. H., Anderson, B. J., Baker, D. N., Benna, M., Boardsen, S. A., et al. (2009). MESSENGER observations of magnetic reconnection in Mercury's magnetosphere. *Science*, *324*(5927), 606–610. https://doi.org/10.1126/science.1172011

Slavin, J. A., Acuña, M. H., Anderson, B. J., Baker, D. N., Benna, M., Gloeckler, G., et al. (2008). Mercury's magnetosphere after MESSENGER's first flyby. *Science*, *321*(5885), 85–89. https://doi.org/10.1126/science.1159040

Slavin, J. A., Anderson, B. J., Baker, D. N., Benna, M., Boardsen, S. A., Gloeckler, G., et al. (2010). MESSENGER observations of extreme loading and unloading of Mercury's magnetic tail. *Science*, *329*(5992), 665–668. https://doi.org/10.1126/science.1188067

Slavin, J. A., DiBraccio, G. A., Gershman, D. J., Imber, S. M., Poh, G. K., Raines, J. M., et al. (2014). MESSENGER observations of Mercury's dayside magnetosphere under extreme solar wind conditions. *Journal of Geophysical Research: Space Physics*, *119*, 8087–8116. https://doi.org/10.1002/2014JA020319

Slavin, J. A., & Holzer, R. E. (1979). The effect of erosion on the solar wind stand-off distance at Mercury. *Journal of Geophysical Research*, *84*(A5), 2076–2082. https://doi.org/10.1029/JA084iA05p02076

Slavin, J. A., Imber, S. M., Boardsen, S. A., DiBraccio, G. A., Sundberg, T., Sarantos, M., et al. (2012). MESSENGER observations of a flux-transfer-event shower at Mercury. *Journal of Geophysical Research*, *117*, A00M06. https://doi.org/10.1029/2012JA017926

Slavin, J. A., Krimigis, S. M., Acuña, M. H., Anderson, B. J., Baker, D. N., Koehn, P. L., et al. (2007). MESSENGER: Exploring Mercury's magnetosphere. *Space Science Reviews*, *131*(1–4), 133–160. https://doi.org/10.1007/s11214-007-9154-x

Slavin, J. A., Lepping, R. P., Wu, C.-C., Anderson, B. J., Baker, D. N., Benna, M., et al. (2010). MESSENGER observations of large flux transfer events at Mercury. *Geophysical Research Letters*, *37*, L02105. https://doi.org/10.1029/2009GL041485

Slavin, J. A., Middleton, H. R., Raines, J. M., Jia, X., Zhong, J., Sun, W.-J., et al. (2019). MESSENGER observations of disappearing dayside magnetosphere events at Mercury. *Journal of Geophysical Research: Space Physics*, *124*, 6613–6635. https://doi.org/10.1029/2019JA026892

Slavin, J. A., Smith, M. F., Mazur, E. L., Baker, D. N., Hones, E. W. Jr., Iyemori, T., & Greenstadt, E. W. (1993). ISEE 3 observations of traveling compression regions in the Earth's magnetotail. *Journal of Geophysical Research*, *98*(A9), 15,425–15,446. https://doi.org/10.1029/93JA01467

Smith, A. W., Jackman, C. M., Frohmaier, C. M., Coxon, J. C., Slavin, J. A., & Fear, R. C. (2018). Evaluating single-spacecraft observations of planetary magnetotails with simple Monte Carlo simulations: 1. Spatial distributions of the neutral line. *Journal of Geophysical Research: Space Physics*, *123*, 10,109–10,123. https://doi.org/10.1029/2018JA025958

Smith, A. W., Jackman, C. M., Frohmaier, C. M., Fear, R. C., Slavin, J. A., & Coxon, J. C. (2018). Evaluating single spacecraft observations of planetary magnetotails with simple Monte Carlo simulations: 2. Magnetic flux rope signature selection effects. *Journal of Geophysical Research: Space Physics*, *123*, 10,124–10,138. https://doi.org/10.1029/2018JA025959

Smith, A. W., Slavin, J. A., Jackman, C. M., Fear, R. C., Poh, G.-K., DiBraccio, G. A., et al. (2017). Automated force-free flux rope identification. *Journal of Geophysical Research: Space Physics*, *122*, 780–791. https://doi.org/10.1002/2016JA022994

Smith, A. W., Slavin, J. A., Jackman, C. M., Poh, G.-K., & Fear, R. C. (2017). Flux ropes in the Hermean magnetotail: Distribution, properties, and formation. *Journal of Geophysical Research: Space Physics*, *122*, 8136–8153. https://doi.org/10.1002/2017JA024295

Solomon, S. C., McNutt, R. L., Gold, R. E., & Domingue, D. L. (2007). MESSENGER mission overview. *Space Science Reviews*, *131*(1–4), 3–39. https://doi.org/10.1007/s11214-007-9247-6

Sonnerup, B. U. Ö., & Scheible, M. (1998). Minimum and maximum variance analysis. In G. Paschmann & P. W. Daly (Eds.), *Analysis methods for multi-spacecraft data* (pp. 185–220). Noordwijk, Netherlands: ESA publication.

Sun, W. J., Slavin, J. A., Fu, S., Raines, J. M., Zong, Q. G., Imber, S. M., et al. (2015). MESSENGER observations of magnetospheric substorm activity in Mercury's near magnetotail. *Geophysical Research Letters*, *42*, 3692–3699. https://doi.org/10.1002/2015GL064052

Sun, W. J., Slavin, J. A., Tian, A. M., Bai, S. C., Poh, G. K., Akhavan-Tafti, M., et al. (2019). MMS study of the structure of ion-scale flux ropes in the Earth's cross-tail current sheet. *Geophysical Research Letters*, *46*, 6168–6177. https://doi.org/10.1029/2019GL083301

Swisdak, M., Opher, M., Drake, J. F., & Alouani Bibi, F. (2010). The vector direction of the intersterllar magnetic field outside the heliosphere. *The Astrophysical Journal*, *710*(2), 1769–1775. https://doi.org/10.1088/0004-637x/710/2/1769

Walker, R. J., & Russell, C. T. (1985). Flux transfer events at the Jovian magnetopause. *Journal of Geophysical Research*, *90*(A8), 7397–7404. https://doi.org/10.1029/JA090iA08p07397

Wang, Y. L., Elphic, R. C., Lavraud, B., Taylor, M. G. G. T., Birn, J., Russell, C. T., et al. (2006). Dependence of flux transfer events on solar wind conditions from 3 years of cluster observations. *Journal of Geophysical Research*, *111*, A04224. https://doi.org/10.1029/2005JA011342

Winslow, R. M., Anderson, B. J., Johnson, C. L., Slavin, J. A., Korth, H., Purucker, M. E., et al. (2013). Mercury's magnetopause and bow shock from MESSENGER magnetometer observations. *Journal of Geophysical Research: Space Physics*, *118*, 2213–2227. https://doi.org/10.1002/jgra.50237

Zhou, H., Tóth, G., Jia, X., Chen, Y., & Markidis, S. (2019). Embedded kinetic simulation of Ganymede's magnetosphere: Improvements and inferences. *Journal of Geophysical Research: Space Physics*, *124*, 5441–5460. https://doi.org/10.1029/2019JA026643